



HAL
open science

Toxicological impact of acute exposure to E171 food additive and TiO₂ nanoparticles on a co-culture of Caco-2 and HT29-MTX intestinal cells

Marie Dorier, Céline Tisseyre, Fanny Dussert, David Béal, Marie-Edith Arnal, Thierry Douki, Vanessa Valdiglesias, Blanca Laffon, Sonia Fraga, Fatima Brandao, et al.

► To cite this version:

Marie Dorier, Céline Tisseyre, Fanny Dussert, David Béal, Marie-Edith Arnal, et al.. Toxicological impact of acute exposure to E171 food additive and TiO₂ nanoparticles on a co-culture of Caco-2 and HT29-MTX intestinal cells. *Mutation Research - Genetic Toxicology and Environmental Mutagenesis*, 2019, 845, pp.402980. 10.1016/j.mrgentox.2018.11.004 . hal-01978322

HAL Id: hal-01978322

<https://hal.science/hal-01978322>

Submitted on 13 Feb 2019

HAL is a multi-disciplinary open access archive for the deposit and dissemination of scientific research documents, whether they are published or not. The documents may come from teaching and research institutions in France or abroad, or from public or private research centers.

L'archive ouverte pluridisciplinaire **HAL**, est destinée au dépôt et à la diffusion de documents scientifiques de niveau recherche, publiés ou non, émanant des établissements d'enseignement et de recherche français ou étrangers, des laboratoires publics ou privés.

Toxicological impact of acute exposure to E171 food additive and TiO₂ nanoparticles on a co-culture of Caco-2 and HT29-MTX intestinal cells

Marie Dorier¹, Céline Tisseyre¹, Fanny Dussert¹, David Béal¹, Marie-Edith Arnal¹, Thierry Douki¹, Vanessa Valdiglesias², Blanca Laffon², Sónia Fraga^{3,4}, Fátima Brandão^{3,4}, Nathalie Herlin-Boime⁵, Frédérick Barreau⁶, Thierry Rabilloud⁷, Marie Carriere^{1,*}

¹ Univ. Grenoble-Alpes, CEA, CNRS, INAC-SyMMES, Chimie Interface Biologie pour l'Environnement, la Santé et la Toxicologie (CIBEST), 38000 Grenoble, France.

² Universidade da Coruña, DICOMOSA Group, Department of Psychology, Area of Psychobiology, Edificio de Servicios Centrales de Investigación, Campus Elviña s/n, 15071-A Coruña, Spain.

³ National Institute of Health, Dept. of Environmental Health, Porto, Portugal

⁴ EPIUnit – Institute of Public Health, University of Porto, Porto, Portugal

⁵ NIMBE, CEA, CNRS, Université Paris-Saclay, CEA Saclay 91191 Gif-sur-Yvette France.

⁶ INSERM, UMR 1220, Institut de Recherche en Santé Digestive, Toulouse, France.

⁷ ProMD, UMR CNRS 5249, CEA Grenoble, DRF/BIG/CBM, Laboratory of Chemistry and Biology of Metals, 38000 Grenoble, France.

*Correspondence: Dr. Marie Carriere, marie.carriere@cea.fr, CEA-Grenoble

INAC/SyMMES/LAN, 17 rue des Martyrs 38054 Grenoble Cedex, France. Phone +33 4 38 78 03 28; Fax: +33 4 38 78 50 90

Declarations of interest: none

Abstract

TiO₂ particles are widely used in products for everyday consumption, such as cosmetics and food; their possible adverse effects on human health must therefore be investigated. The aim of this study was to document *in vitro* impact of the food additive E171, i.e. TiO₂, and of TiO₂ nanoparticles, on a co-culture of Caco-2 and HT29-MTX cells, which is an *in vitro* model for human intestine. Cells were exposed to TiO₂ particles three days after seeding, i.e. while they were not fully differentiated. Cell viability, reactive oxygen species (ROS) levels and DNA integrity were assessed, by MTT assay, DCFH-DA assay, alkaline and Fpg-modified comet assay and 8-oxo-dGuo measurement by HPLC-MS/MS. The mRNA expression of genes involved in ROS regulation, DNA repair via base-excision repair, and endoplasmic reticulum stress was assessed by RT-qPCR. Exposure to TiO₂ particles resulted in increased intracellular ROS levels, but did not impair cell viability and did not cause any oxidative damage to DNA. Only minor changes in mRNA expression were detected. Altogether, this shows that E171 food additive and TiO₂ nanoparticles only produce minor effects to this *in vitro* intestinal cell model.

Keywords: nanoparticle, TiO₂, E171, food additive, toxicity, intestine

1. Introduction

TiO₂ has been used for more than 50 years as a food additive, under the code E171 within the European Union. Indeed, because of its low toxicity and intestinal absorption, E171 has been authorized since the '60ies without any established acceptable limitation of daily intake, in Europe [1]. It is primarily used as a whitening agent and as an opacifier in pastries and sweets [2, 3]. E171 is not a nanomaterial according to the EU Recommendation on the definition of a nanomaterial (Official Journal of the European Union (2011/696/EU) 18/10/2011), because it contains less than 50% of particles, in the number size distribution, with at least one diameter below 100 nm, i.e., nanoparticles (NPs) [2, 4-6]. It is made of particles with average diameter around 100-200 nm, with a high polydispersity. Its crystal structure is mainly anatase although some samples were shown to be rutile [5, 6]; and it sometimes contains 0.5-1.8 mg phosphorous (P)/g of TiO₂ [6].

Several reports published during the past 2 years address the questions of toxicity and absorption of E171. A single dosing of seven human volunteers to 100 mg of E171, ingested as gelatin capsules, resulted in translocation of TiO₂ particles to the bloodstream, with maximal absorption 6 h after administration [7]. Given the observed kinetics, there may be two routes of absorption from the human intestinal lumen, one proximal and one distal [7]. The authors of this study did not report any toxicity that may be associated with ingestion of E171. *In vivo*, in a colitis-associated mouse model, E171 administered by oral gavage at 5 mg/kg b.w. per day, 5 days a week, for 10 weeks, enhanced the formation of colon tumors and exacerbated tumor progression and colon inflammation [8]. The same authors did not report any tumor formation in non-chemically induced mice exposed to E171, but some dysplastic changes in colonic epithelium were reported, as well as decrease in the number of goblet cells [8]. In the distal colon of these mice, gene expression profiling showed that E171 regulated

the mRNA expression of GPCR/olfactory and serotonin gene receptors, induced mRNA expression of genes encoding proteins involved in oxidative stress, immune response pathways, and DNA repair. Moreover exposure to E171 both up- and down-regulated genes encoding proteins involved in the development of cancer [9]. In rats, low doses of E171 administered either by intragastric gavage for 7 days or via drinking water for 100 days (10 mg/kg b.w. per day) impaired immune homeostasis; they initiated and promoted the expansion of preneoplastic lesions in the colon, although their number was low, and concomitantly induced the development of a low-grade inflammatory microenvironment in the mucosa [10]. *In vitro*, repeated exposure to E171 of a co-culture of Caco-2 and HT29-MTX for 21 days induced accumulation of reactive oxygen species (ROS) and oxidized DNA bases, but did not lead to cell mortality, DNA strand break or endoplasmic reticulum stress [4]. Oxidized bases in DNA, especially 8-oxo-dGuo, are known to be mutagenic, because they can pair with adenine (A) or cytosine (C) with equal efficiency, thus leading to G:C to thymine (T):A transversion [11]. They may thus explain the carcinogenicity of E171 reported by Bettini et al [10]. Finally, also in an *in vitro* experiment, Proquin et al. reported that E171 causes ROS accumulation in undifferentiated Caco-2 cells, together with single strand breaks and/or alkali-labile sites in DNA, as probed via the comet assay [12]. Moreover it induced chromosomal damage in HCT116 cells, as probed via the cytokinesis-block micronucleus assay [12].

We aimed here at evaluating the toxicological impact of E171 and two model TiO₂-NPs, A12 (anatase, 12 nm) and NM105 from the Joint Research Center at the European Commission (anatase/rutile, 24 nm), on a co-culture of Caco-2 (enterocytic-like) and HT29-MTX (mucus-secreting) cells. To recapitulate a mucus-secreting intestinal epithelium, the co-culture of Caco-2 and HT29-MTX cells is usually grown for 21 days post-confluence, to allow cells to differentiate. Here we used this model three days post-seedling; in this condition cells are not

fully differentiated. Contrary to differentiated Caco-2 cells, undifferentiated Caco-2 cells do not express all the biochemical and morphological characteristics of human enterocytes. Their phenotype is that of proliferating cells. In this condition, according to previous studies, their sensitivity towards NPs is higher than that of differentiated Caco-2 cells [13, 14]. Conversely, three days post-seeding, HT29-MTX cells already produce some mucus. This cell model was acutely exposed for 6 h, 24 h or 48 h to A12, NM105 or E171. Cell viability, oxidative DNA damage and ROS accumulation were investigated since oxidative stress is one of the main mechanisms of TiO₂ particle toxicity. In addition, impact of E171 and TiO₂-NPs on actors of the UPR pathway, which is activated in ER stress condition [15], was also investigated because NP toxicity through ER stress signaling pathway has previously been reported [16-18] and because ER stress is closely related to oxidative stress [19]. Finally, impact on mRNA expression of DNA repair proteins was investigated by RT-qPCR.

Our results show that E171 was not cytotoxic even at high concentrations, but caused ROS accumulation in exposed cells, whatever the dose. E171 did not have major impact on DNA integrity, and did not significantly modulate the mRNA expression of proteins involved in DNA repair, in antioxidant defense system and in the UPR pathway. Consequently, these results suggest that TiO₂, either micro- or nano-sized, exhibits minor effects on this *in vitro* intestinal cell model.

2. Material and Methods

2.1. Chemicals and reagents

Unless otherwise indicated, chemicals were all purchased from Sigma-Aldrich and were >99 % pure. Cell culture media and serum were purchased from Thermo Fisher Scientific.

2.2. Particle dispersion and characterization

E171 was obtained from a French supplier of food coloring for bakeries. A12 was synthesized in our laboratories [20], it has already been used in our previous studies [4, 21, 22]. NM105 was provided by the nanomaterial library at the European Joint Research Center (JRC, Ispra, Italy). These particles were fully characterized, as reported in our previous article [4]. Briefly, mean primary diameter of E171, A12 and NM105 were 118 ± 53 nm, 12 ± 3 nm and 24 ± 6 nm, respectively. Their SSA was 9.4, 82 and 46 m²/g, respectively. Particles were then weighted in 15 ml polypropylene vials, and suspended in ultrapure sterile water at a concentration of 10 mg/mL. We chose to disperse particles by sonication in water rather than in cell culture medium, because sonication of proteins from fetal bovine serum (FBS) would cause their agglomeration [23], creating large aggregates that would hinder particle detection by dynamic light scattering (DLS). Moreover protein aggregates may alter cellular endocytosis and/or particle coating. Particles were sonicated for 30 min at 80% of amplitude, 4 °C (Huber minichiller), using high energy sonication (Bioblock Scientific, Vibracell 75041) with an indirect cup-type sonicator (Cup Horn), immediately before cell exposure. The power of this sonicator was measured using the calorimetric procedure [24]; 80% of amplitude corresponds to 47.7 W. In this condition, hydrodynamic diameter and polydispersity index (PdI) of E171, A12 and NM105 were 415 ± 69 (PdI: 0.48 ± 0.07), 85 ± 3 (PdI: 0.17 ± 0.02) and 158 ± 1 (PdI: 0.16 ± 0.01), respectively [4]. For cell exposure they were then diluted in cell culture medium

containing FBS, as proteins from FBS would create a protein corona which would prevent particle agglomeration. After dilution in cell culture medium, hydrodynamic diameter and PDI of E171, A12 and NM105 was 739 ± 355 nm (PDI: 0.64 ± 0.22), 448 ± 1 nm (PDI: 0.25 ± 0.02) and 440 ± 7 nm (PDI: 0.18 ± 0.01), respectively [4]. Zeta potential was -19 ± 1 mV, -11 ± 1 mV and -11 ± 1 mV, respectively [4].

2.3. Cell culture and exposure to TiO₂ particles

Caco-2 cells (ATCC HTB-37, passages from 49 to 60), Caco-2 cells transfected with EGFP-encoding lentivirus, which stably express EGFP (Caco-2-GFP, developed by F. Barreau, passages from 9 to 15) and HT29-MTX mucus-secreting cells (kindly provided by T. Lesuffleur, INSERM U843, Paris, France, passages from 21 to 35) were maintained, in separate flasks, in Dulbecco's Modified Eagle Medium + GlutaMAX™ supplemented with 10% heat inactivated FBS, 1% non-essential amino acids (NEAA), 50 units/ml penicillin and 50 µg/ml streptomycin. They were maintained at 37°C under 5% CO₂. For the following experiments, cells were then seeded as a co-culture composed of 70% Caco-2 and 30% HT29-MTX cells, at a density of 24 000 cells/cm², in 60 cm² petri dishes or multi-well plates. Three days post-seeding, cells were exposed to TiO₂ particles diluted in cell culture medium (containing 10% of FBS) for 6 h, 24 h or 48 h.

2.4. Characterization of Caco-2/HT29-MTX co-culture by fluorescence activated cell sorting (FACS)

The proportion of Caco-2 and HT29-MTX in the co-culture was monitored 6 h, 48 h and 72 h after seeding (i.e. during the three days preceding exposure to TiO₂), using Caco-2-GFP cells that enable the sorting of green cells (Caco-2-GFP) and non-fluorescent cells (HT29-MTX)

by FACS. As for other experiments, Caco-2-GFP and HT29-MTX cells were grown separately, then harvested and seeded in 56-cm² petri dishes at a density of 24 000 cells per cm². Immediately after seeding, 3 vials containing 1 million cells each were fixed with 4% (w/v) paraformaldehyde for 15 min at room temperature, then washed twice with PBS. Then, 6 h, 48 h and 72 h after seeding, cells were harvested with trypsin (3 petri dishes per time point), fixed with 4% (w/v) paraformaldehyde for 15 min at room temperature, washed twice with PBS. Samples were stored at 4°C until analysis, on a FACS Calibur instrument (Becton Dickinson).

2.4. Toxicity assays

2.4.1. Cell viability

After acute exposure to E171 and TiO₂-NPs, cell viability was assessed via the 3-(4,5-dimethylthiazol-2-yl)-2,5-diphenyl-tetrazolium bromide (MTT) assay, which measures metabolic activity. Cells were grown in 96-wells plates and exposed to 0-200 µg/mL of particles for 6 h or 48 h. Then exposure medium was discarded and replaced by 100 µL of 0.5 mg/mL MTT solution. After 2 h of incubation at 37°C, the MTT solution was discarded and formazan crystals were dissolved in 100 µL DMSO. Interferences of particles with the assay were tested as previously described [21] (Table S1). Since optical interference of TiO₂ particles was detected, after dissolution of formazan crystals, the plates were centrifuged for 5 min at 500 rpm, then 50 µL of supernatants was transferred to a clean plate, and absorbance at 550 nm was measured (SpectraMax M2, Molecular Devices). In this condition, no interference is observed (Figure S1).

2.4.2. Reactive Oxygen Species (ROS) measurement

Intracellular ROS content was assessed using 2',7'-dichlorodihydrofluorescein diacetate acetyl ester (DCFH-DA) (Invitrogen). After exposure to particles, cells were rinsed twice with PBS and incubated with 80 μ M DCFH-DA (Life Technologies), prepared in complete cell culture medium, for 30 min at 37°C. They were harvested by scraping, and DCF fluorescence intensity was measured at $\lambda_{exc}/\lambda_{em}$ 480 nm/570 nm (SpectraMax M2, Molecular Devices). After background removal ($\lambda_{exc}/\lambda_{em}$ 480 nm/650 nm), DCF fluorescence was normalized to protein concentration. Potential interference of particle was tested, by measuring the fluorescence of cells exposed to particles but not with DCFH-DA, and by measuring the fluorescence of particles suspensions (10-50-100 μ g/mL) mixed with DCFH-DA (no cells). No interference was detected (table S2).

2.4.3. Comet assay

DNA strand breaks and alkali-labile sites were assessed through the alkaline version of the comet assay. Fpg-sensitive sites, including 8-oxo-dGuo, were quantified by incubating the slides with formamidopyrimidine-DNA glycosylase enzyme (Fpg). Cells were exposed to TiO₂ particles in 24-well plates. After exposure, they were collected and stored at -80°C in citrate buffer (11.8 g/L) containing sucrose (85.5 g/L) and DMSO (50 mL/L), pH 7.6.

Approximately 10000 cells were mixed with low melting point agarose (0.6% in PBS) and dropped on slides previously coated with standard 1% agarose (n=6). After solidification on ice for 10 min, slides were placed in cold lysis buffer (2.5 M NaCl, 100 mM EDTA, 10 mM Tris, 10% DMSO, 1% Triton X-100, pH10) and incubated overnight at 4°C. They were then rinsed in 0.4 M Tris pH 7.4. For each individual biological replicate, three slides were incubated with Fpg buffer (Invitrogen), and 3 slides were incubated with 100 μ L of Fpg (Trevigen, 5 U/slide) prepared in Fpg buffer, for 45 min at 37 °C. DNA was then allowed to

unwind for 30 min in electrophoresis buffer (0.3 M NaOH, 1 mM EDTA), followed by electrophoresis in a vertical comet assay tank (COMPAC50, Cleaver Scientific) at 21 V (1 V/cm) for 30 min. After neutralization in 0.4 M Tris pH 7.4, comets were stained with 50 μ L of GelRed (Life Technologies). As positive control for alkaline comet assay, cells were exposed for 24 h to 30 μ g/mL of methyl-methanesulfonate (MMS). As positive control for comet-Fpg, we used A549 cells exposed to 1 μ M riboflavin for 20 min at 37 °C, then irradiated with 10 J/cm² of UVA. As positive control for electrophoresis, 50 μ M of H₂O₂ was deposited on an extra slide of control cells and incubated for 5 min on ice (not shown). Comets were scored using image analysis Comet IV software (Perceptive Instruments, Suffolk, UK), and median % DNA in tail was calculated for at least 50 comets per slide. Net pgsensitive sites (Net Fpg) were calculated as the difference in % DNA in tail between samples with Fpg incubation and samples with buffer incubation. The whole experiment was repeated three times independently (n=3).

2.4.4. 53BP1 foci count

The number of p53-binding protein 1 (53BP1) foci per cell nuclei was evaluated by immunostaining of cells fixed for 15 min in 4% paraformaldehyde and permeabilized for 15 min in 0.1% triton X-100, using anti-53BP1 antibody (Abnova, 1/2000, vol./vol., exposure 1 h at room temperature) and anti-rabbit secondary antibody coupled to Atto488 (1/1000, exposure 1 h at room temperature). Cell nuclei were then stained for 15 min with Hoechst 33342 (1 μ g.ml⁻¹). As positive control, cells were exposed to 50 μ M of etoposide for 24 h. Total number of 53BP1 foci was automatically counted, as well as total number of nuclei, using a Cell Insight CX5 (Thermofisher); data were analyzed using the SpotDetector v4 Bioapplication.

2.4.5. HPLC/MS-MS for 8-oxo-dGuo measurement

8-oxodGuo was quantified by HPLC-tandem mass spectrometry (HPLC-MS/MS) [25]. DNA was extracted and digested as described by Ravanat et al. [26]. Briefly, a lysis buffer containing Triton X-100 was added to the cellular pellet. The nuclei were collected by centrifugation and further lysed in a Tris-EDTA buffer to which 10% SDS was added. The samples were incubated with a mixture of RNase A and RNase T1, and subsequently treated by proteinase. DNA was precipitated using isopropanol and concentrated sodium iodide. Deferoxamine was added to all buffers to prevent spurious oxidation. DNA was then digested into a mixture of nucleosides, first by incubation with nuclease P1, DNase II and phosphodiesterase II at pH 6, for 2 h. They were then further digested in alkaline phosphatase and phosphodiesterase I, pH 8, for 2 h. The solution was neutralized with 0.1 μ M HCl and centrifuged. The supernatant was collected and injected onto the HPLC-MS/MS system. 8-OxodGuo was quantified with an ExionLC HPLC system connected to a QTRAP 6500+ mass spectrometer (SCIEX). The spectrometer was used in the MRM³ mode with positive electrospray ionization. The monitored fragmentation was m/z 284 $[M + H]^+ \rightarrow 168 [M + H - 2\text{-deoxyribose}]^+ \rightarrow 140 [M + H - 2\text{-deoxyribose-CO}]^+$. Chromatographic separations were achieved using a C18 reversed phase Uptisphere ODB column (Interchim, Montluçon, France). The elution was performed using a gradient of acetonitrile in 2 mM ammonium formate, at a flow rate of 0.2 mL/min. The retention time was 20 min. In addition to the MS spectrometer, the HPLC eluent was analyzed in a UV detector set at 270 nm to quantify the amount of unmodified nucleosides. Levels of 8-oxodGuo were expressed as number of lesions per million normal bases.

2.4.6. Gene expression

Gene expression was measured by real-time-quantitative polymerase chain reaction (RT-qPCR). RNA was extracted using GenElute™ mammalian total RNA Miniprep assay. Cells were harvested in lysis buffer from the Miniprep assay and stored at -80°C. The integrity of RNA was checked by measurement of absorbance at 260, 280 and 230 using a Nanodrop ND-1000 (Thermofisher), and calculation of abs 260/abs 280 and abs 260/abs 230 nm ratios. 2 µg of total RNA was reverse transcribed to cDNA with 100 ng/µL random primers, 10 mM dNTP and the SuperScript III Reverse Transcriptase (Invitrogen). Quantitative PCR was run with MESA Blue qPCR Mastermix for SYBR Assay with ROX reference (Eurogentec) in a CFX96 Real time system, C1000 Touch Thermal cycler (Bio-Rad). Primer sequences are reported in Table S3. *S18* and *GAPDH* were used as reference genes for normalization. Variability of their expression was assessed using Bestkeeper, an Excel-based pairwise mRNA correlation tool [27]. Relative gene expression was calculated using the Relative Expression Software Tool (REST2009) [28].

2.5. Statistical analysis

Except for RT-qPCR experiments, statistical analyses were performed using Statistica 8.0 software (Statsoft, Chicago, USA). Unless indicated otherwise, statistical significance was assessed based on a non-parametric one-way analysis of variance on ranks approach (Kruskal-Wallis) followed by pairwise comparison using a Mann-Whitney u-test. Results were considered statistically significant when the p-value was < 0.05.

3. Results

3.1. Characterization of the Caco-2/HT29-MTX co-culture

Caco-2-GFP and HT29-MTX were seeded at the initial ratio of 70:30. After 6 h in culture, which is the time necessary for cells to adhere to the flask, and after 48 h, the proportion was still approximately 70:30 (Figure 1). This proportion changed 72 h after seeding, and reached 77:23 (Figure 1). Consequently, when cells were exposed to TiO₂ particles, the co-culture was composed of 77% Caco-2 and 23% HT29-MTX, which is comparable to the proportion of enterocytes and goblet cells in human colon [29].

3.1. Cytotoxicity

Cells were exposed to E171 or NM105 for 6 h or 48 h. Cell viability was not altered by exposure to E171 or NM105, up to 200 µg/mL (Figure 2). Optical interference of TiO₂ particles with MTT assay was detected, the protocol was therefore adapted to eliminate TiO₂ particles before absorbance measurement.

3.2. Oxidative stress

Whatever the exposure condition, ROS levels were significantly higher in cells exposed to TiO₂ particles, as compared to control cells (Figure 3). This increase in ROS level was not dependent on exposure time, nor on the type of TiO₂ particle (Figure 3A). In cells exposed to E171, increased ROS level was dependent on E171 concentration, with significantly higher ROS levels in cells exposed to 50 or 100 µg/mL of E171, compared to cells exposed to 10 µg/mL of E171, whatever the exposure time (Figure 3B). Possible interaction of TiO₂ particles with H₂-DCF-DA was tested, no interference was detected (Table S2).

Then, the expression of genes encoding proteins involved in antioxidant defense mechanisms, namely catalase (*CAT*), glutathione reductase (*GSR*), superoxide dismutase 1 and 2 (*SOD1*, *SOD2*), was measured by RT-qPCR in cells exposed to TiO₂ particles for 6 h or 48 h. Only very moderate modulation of the mRNA expression was observed, with downregulated mRNA expression of SOD1 and SOD2 in cells exposed for 48 h to E171 or A12, respectively (Table 1). Moreover, there was no significant modulation in mRNA expression level of *NRF2*, a transcription factor implicated in oxidative stress regulation.

3.3. DNA damage

Since intracellular accumulation of ROS could trigger oxidative damage to DNA, DNA integrity was assessed in exposed cells via comet assay (alkaline and Fpg-modified), which probes DNA strand breaks and alkali-labile sites such as abasic sites, as well as Fpg-sensitive sites such as 8-oxo-dGuo; 53BP1 foci count, which probe DNA double strand breaks; then 8-oxo-dGuo was measured by HPLC/MS-MS, as probe of DNA base oxidation. No DNA strand break and/or alkali-labile site was detected in cells exposed to TiO₂ particles via the alkaline version of comet assay, whatever the exposure condition (Figure 4, “SBs+ALB”). No Fpg-sensitive site (and among them 8-oxo-dGuo) was detected in the Fpg-modified version of comet assay (Figure 4, “Net Fpg”). No significant increase in DNA double strand break was detected via 53BP1 foci immunostaining in exposed cells, compared to control cells (Figure 5). Moreover, no significant increase of the 8-oxo-dGuo level was detected by HPLC/MS-MS (Figure 6). We even observed decreased level of 8-oxo-dGuo in cells exposed to P25 or E171 for 6 h. Conversely, positive outcome was observed for positive controls in these assays, i.e. cells exposed to 30 µg/mL of methyl methanesulfoxide for 24 h in the alkaline version of comet assay, cells exposed to riboflavin and irradiated with UVA in the Fpg-modified version

of comet assay, cells exposed to 50 μM of etoposide in the 53BP1 assay, and cells exposed to KBrO_3 in the 8-oxo-dGuo quantification assay.

The mRNA expression of DNA repair proteins, involved in the base excision repair pathway, was monitored via RT-qPCR. No significant gene expression change was detected, except increased expression of GADD45 in cells exposed for 48 h to P25 (Table 1).

3.4. Endoplasmic reticulum stress

The mRNA expression of *IRE-1*, *ATF6*, *sXBP1*, and *GRP78*, which mediate the UPR response, was then analyzed in cells exposed to TiO_2 particles. Again, no significant modulation of mRNA expression was observed (Table 1).

4. Discussion

The objective of the present study was to assess the cytotoxicity, DNA damage, oxidative stress and endoplasmic reticulum stress caused by E171 and TiO_2 nanoparticles on a co-culture of Caco-2 and HT29-MTX cells, seeded at 70% and 30%, respectively. In all experiments, Caco-2 cells were not differentiated, they were thus proliferative; conversely HT29-MTX already produced some mucus. This cell model was exposed to up to 200 $\mu\text{g/mL}$ of TiO_2 , which is a high concentration as compared to the estimated human daily intake [5, 30-32]. TiO_2 particles were prepared in complete cell culture medium, i.e. in the presence of FBS proteins. This particular combination of parameters was chosen to take into account physiological parameters. First, it should be kept in mind that in normal intestinal villi, epithelial cells undergo a differentiation gradient from the bottom of crypts to the top of villi, while always covered by mucus. The differentiation state of cells used here is in accordance

with this physiology. Second, even when ingested without an associated meal, TiO₂ food additive is covered with salivary proteins and gastric enzymes before it enters the intestine. Therefore, the use of FBS proteins in exposure medium, which leads to the formation of a dense protein corona on the surface of NPs, is relevant. Thus, our setup appears to be a valuable addition to the battery of *in vitro* systems used for the estimation of gastrointestinal effects of micro- and nanoparticles.

Our results are in accordance with the published literature which shows that the overall toxicity of TiO₂ is low, even at high concentration [33-35]. They concur with our previous study, where pure anatase and pure rutile TiO₂-NPs were proven to induce only minor impact on undifferentiated Caco-2 cells [22]. They induced no cytotoxicity, no DNA strand breaks or alkali-labile sites, but they caused accumulation of ROS, modulation of GSH level and decreased activity of superoxide dismutase in exposed cells [22]. Our observations also concur with the study published by Song et al. [14] which showed, on undifferentiated Caco-2 cell, that pure anatase TiO₂ particles, either nanoparticles or food-grade particles, induce limited membrane damage and no change in cell proliferation [14], but a dose-dependent increase of ROS level [14].

Proquin et al. previously reported that TiO₂ nanoparticles and E171 induced genotoxic damage to Caco-2 and HCT116 cells, in the alkaline version of comet assay and in the micronucleus assay, respectively [12]. Different hypotheses can explain the discrepant result observed in the present study. First, TiO₂ preparation procedure is different: Proquin et al. dispersed TiO₂ particles in DMEM medium containing 0.05% of bovine serum albumin (BSA), then this suspension of particles was sonicated. Particles were then diluted in culture medium containing FBS. Sonication of proteins is known to cause their denaturation and aggregation [23]. For this reason, we chose to rather disperse TiO₂ particles by sonication in water, then to dilute them immediately in cell culture medium containing FBS because

proteins from serum would hinder particle agglomeration via steric repulsion. Moreover Proquin et al. used bath sonication while we used high energy sonication. Consequently, the dispersion state of particles differs, in these two studies: while we obtained stable suspensions with average hydrodynamic diameter 450 nm for NPs and 750 nm for E171, Proquin et al. obtained suspensions containing large agglomerates (>1000 nm). Different hydrodynamic diameters may induce different exposure levels, with large agglomerates settling down very rapidly on cells and therefore increasing exposure. This would explain the positive outcomes observed by Proquin et al. in genotoxicity testing, while we observed no genotoxicity in our exposure conditions. Another difference is the cell model used here, compared to the study by Proquin et al. We used a co-culture of Caco-2 and HT29-MTX cells while Proquin et al. used Caco-2 cells. HT29-MTX secrete some mucus, which can cover the cells and therefore protect them from NPs. In a previous study, we showed that accumulation of TiO₂-NPs and E171 is similar in a monoculture of Caco-2 cells and in a co-culture of Caco-2 and HT29-MTX cells, exposed 21 days post-seeding, i.e. when cells are fully-differentiated. But the situation may be different in non-differentiated cells, i.e. non-differentiated Caco-2/HT29-MTX co-culture may accumulate more TiO₂ particles than non-differentiated Caco-2 monoculture, which would also explain the discordant results observed here.

Positive outcome in cytotoxicity (LDH and WST-1) and genotoxicity (Fpg-modified version of comet assay) testing was also observed by Gerloff et al., in non-differentiated Caco-2 cells, exposed to mixed anatase/rutile TiO₂-NPs [36, 37]. In the two studies by Gerloff *et al.*, exposure medium was serum-free whereas in our exposure conditions it contained FBS.

According to the literature, the different protein coronas that form on NPs determine particle biological signature, which influences their accumulation and impact on cells [38-40]. A dense protein corona, which forms when particles are diluted in medium containing FBS, has been shown to decrease TiO₂-NPs toxicological impact in cells [13, 38]. This can explain why

Gerloff et al. observed cyto- and genotoxicity while we do not. Again, this discussion underlines the necessity to use similar dispersion procedures and exposure conditions for *in vitro* assessment of nano- and microparticle toxicity so that a consensus is obtained.

The absence of genotoxicity observed *in vitro* may be put into perspective with the recently published *in vivo* data, showing carcinogenic potential of E171 and TiO₂-NPs [10]. In this *in vivo* study, the authors showed the potential of E171 and TiO₂-NPs to initiate preneoplastic lesions and to induce the growth of aberrant crypt foci [10]. These observations were concomitant with absence of *in vivo* genotoxicity in the colon mucosa, but coincided with promotion of colon micro-inflammation [10]. TiO₂ particles may therefore be classified in the group of promoters of carcinogens that induce cancer via non-genotoxic mechanisms [41]. Since both micro-inflammation and immune homeostasis disruption were observed in this *in vivo* study, the mechanisms of this non-genotoxic carcinogenicity may occur either via immunosuppression or via the promotion of a dysregulated inflammatory response [41]. This is consistent with the hypothesis of Vales et al., who showed in BEAS-2B bronchial epithelial cells, that chronic exposure to low doses of TiO₂-NPs causes cell transformation and acquisition of a cancer phenotype, without causing any primary genotoxicity or chromosomal damage [42]. We used a co-culture of epithelial intestinal cells, with no immune cells which are the main actors of the inflammatory response, and which may lead to secondary genotoxicity. Therefore, our model is not the best one when investigating secondary genotoxicity caused by NPs. An *in vitro* 3D model combining epithelial cells and immune cells has been developed recently [43], it would be a better model to assess inflammation and secondary genotoxicity.

Acute exposure to TiO₂ particles causes accumulation of ROS but no oxidative damage to DNA and unchanged mRNA levels of redox enzymes and of NRF-2. This suggests that cells would scavenge these ROS thanks to already existing enzymes or antioxidant molecules such

as glutathione. Therefore TiO₂ particles, either nanoparticles or E171 food additive cause only minor toxicological impact on this *in vitro* intestinal model.

5. Conclusion

TiO₂ toxicity was evaluated *in vitro*, on a model mucus-secreting intestinal epithelium in which enterocytes are not fully differentiated and still proliferative. Both TiO₂ nanoparticles and E171 food additive increased intracellular ROS level, in a dose-dependent manner for E171. They did not induce any loss of cell viability, or impairment of DNA integrity, or endoplasmic reticulum stress. At current exposure conditions, this shows that E171 food additive and TiO₂ nanoparticles only produce minor effects to this *in vitro* intestinal cell model.

6. Acknowledgments

This work was supported by Atomic Energy and Alternative Energies Commission (CEA) through the ‘Toxicology’ research program (IMAGINATOX grant); the French Environment and Energy Management Agency (ADEME); the French Agency for Food, Environmental and Occupational Health & Safety (ANSES) within the framework of the National Research Program for Environmental and Occupational Health (PNR-EST, EST-2013/1/024, NanoGut grant) and the French National Research Agency (ANR, ANR-16-CE34-0011-01, PAIPITO grant). It is a contribution to the Labex Serenade (ANR-11-LABX-0064) funded by the French Government’s “Investissements d’Avenir” ANR program, through the A*MIDEX project (ANR-11-IDEX-0001-02). It has been performed in the frame of the hCOMET COST action (CA15132). The authors would like to thank T. Lesuffleur (INSERM U938, Paris, France) for generous gift of HT29-MTX cells.

7. References

- [1] B. Jovanovic, Critical review of public health regulations of titanium dioxide, a human food additive, *Integrated environmental assessment and management*, 11 (2015) 10-20.
- [2] R.J. Peters, G. van Bommel, Z. Herrera-Rivera, H.P. Helsper, H.J. Marvin, S. Weigel, P.C. Tromp, A.G. Oomen, A.G. Rietveld, H. Bouwmeester, Characterization of titanium dioxide nanoparticles in food products: analytical methods to define nanoparticles, *Journal of agricultural and food chemistry*, 62 (2014) 6285-6293.
- [3] R.J.B. Peters, H. Bouwmeester, S. Gottardo, V. Amenta, M. Arena, P. Brandhoff, H.J.P. Marvin, A. Mech, F.B. Moniz, L.Q. Pesudo, H. Rauscher, R. Schoonjans, A.K. Undas, M.V. Vettori, S. Weigel, K. Aschberger, Nanomaterials for products and application in agriculture, feed and food, *Trends in Food Science & Technology*, 54 (2016) 155-164.
- [4] M. Dorier, D. Beal, C. Marie-Desvergne, M. Dubosson, F. Barreau, Continuous in vitro exposure of intestinal epithelial cells to E171 food additive causes oxidative stress, inducing oxidation of DNA bases but no endoplasmic reticulum stress, *Nanotoxicology*, 11 (2017) 751-761.
- [5] A. Weir, P. Westerhoff, L. Fabricius, K. Hristovski, N. von Goetz, Titanium dioxide nanoparticles in food and personal care products, *Environmental science & technology*, 46 (2012) 2242-2250.
- [6] Y. Yang, K. Doudrick, X. Bi, K. Hristovski, P. Herckes, P. Westerhoff, R. Kaegi, Characterization of food-grade titanium dioxide: the presence of nanosized particles, *Environmental science & technology*, 48 (2014) 6391-6400.
- [7] L.C. Pele, V. Thoree, S.F. Bruggraber, D. Koller, R.P. Thompson, M.C. Lomer, J.J. Powell, Pharmaceutical/food grade titanium dioxide particles are absorbed into the bloodstream of human volunteers, *Particle and fibre toxicology*, 12 (2015) 26.

- [8] I.M. Urrutia-Ortega, L.G. Garduno-Balderas, N.L. Delgado-Buenrostro, V. Freyre-Fonseca, J.O. Flores-Flores, A. Gonzalez-Robles, J. Pedraza-Chaverri, R. Hernandez-Pando, M. Rodriguez-Sosa, S. Leon-Cabrera, L.I. Terrazas, H. van Loveren, Y.I. Chirino, Food-grade titanium dioxide exposure exacerbates tumor formation in colitis associated cancer model, *Food and Chemical Toxicology*, 93 (2016) 20-31.
- [9] H. Proquin, M.J. Jetten, M.C.M. Jonkhout, L.G. Garduno-Balderas, J.J. Briede, T.M. de Kok, Y.I. Chirino, H. van Loveren, Gene expression profiling in colon of mice exposed to food additive titanium dioxide (E171), *Food and chemical toxicology*, 111 (2018) 153-165.
- [10] S. Bettini, E. Boutet-Robinet, C. Cartier, C. Comera, E. Gaultier, J. Dupuy, N. Naud, S. Tache, P. Grysan, S. Reguer, N. Thieriet, M. Refregiers, D. Thiaudiere, J.P. Cravedi, M. Carriere, J.N. Audinot, F.H. Pierre, L. Guzylack-Piriou, E. Houdeau, Food-grade TiO₂ impairs intestinal and systemic immune homeostasis, initiates preneoplastic lesions and promotes aberrant crypt development in the rat colon, *Scientific reports*, 7 (2017) 40373.
- [11] M. Carriere, S. Sauvaigo, T. Douki, J.L. Ravanat, Impact of nanoparticles on DNA repair processes: current knowledge and working hypotheses, *Mutagenesis*, 32 (2017) 203-213.
- [12] H. Proquin, C. Rodriguez-Ibarra, C.G. Moonen, I.M. Urrutia Ortega, J.J. Briede, T.M. de Kok, H. van Loveren, Y.I. Chirino, Titanium dioxide food additive (E171) induces ROS formation and genotoxicity: contribution of micro and nano-sized fractions, *Mutagenesis*, 32 (2017) 139-149.
- [13] K. Gerloff, D.I. Pereira, N. Faria, A.W. Boots, J. Kolling, I. Forster, C. Albrecht, J.J. Powell, R.P. Schins, Influence of simulated gastrointestinal conditions on particle-induced cytotoxicity and interleukin-8 regulation in differentiated and undifferentiated Caco-2 cells, *Nanotoxicology*, 7 (2013) 353-366.

- [14] Z.M. Song, N. Chen, J.H. Liu, H. Tang, X. Deng, W.S. Xi, K. Han, A. Cao, Y. Liu, H. Wang, Biological effect of food additive titanium dioxide nanoparticles on intestine: an in vitro study, *Journal of applied toxicology*, 35 (2015) 1169-1178.
- [15] M.A. McGuckin, R.D. Eri, I. Das, R. Lourie, T.H. Florin, ER stress and the unfolded protein response in intestinal inflammation, *American Journal of Physiology-Gastrointestinal and Liver Physiology*, 298 (2010) G820-G832.
- [16] V. Christen, M. Camenzind, K. Fent, Silica nanoparticles induce endoplasmic reticulum stress response, oxidative stress and activate the mitogen-activated protein kinase (MAPK) signaling pathway, *Toxicology Reports*, 1 (2014) 1143–1151.
- [17] K.N. Yu, S.H. Chang, S.J. Park, J. Lim, J. Lee, T.J. Yoon, J.S. Kim, M.H. Cho, Titanium Dioxide Nanoparticles Induce Endoplasmic Reticulum Stress-Mediated Autophagic Cell Death via Mitochondria-Associated Endoplasmic Reticulum Membrane Disruption in Normal Lung Cells, *PloS one*, 10 (2015) e0131208.
- [18] R. Zhang, M.J. Piao, K.C. Kim, A.D. Kim, J.Y. Choi, J. Choi, J.W. Hyun, Endoplasmic reticulum stress signaling is involved in silver nanoparticles-induced apoptosis, *The international journal of biochemistry & cell biology*, 44 (2012) 224-232.
- [19] J.D. Malhotra, R.J. Kaufman, Endoplasmic reticulum stress and oxidative stress: a vicious cycle or a double-edged sword?, *Antioxidants & redox signaling*, 9 (2007) 2277-2293.
- [20] B. Pignon, H. Maskrot, V.G. Ferreol, Y. Leconte, S. Coste, M. Gervais, T. Pouget, C. Reynaud, J.F. Tranchant, N. Herlin-Boime, Versatility of laser pyrolysis applied to the synthesis of TiO₂ nanoparticles - Application to UV attenuation, *European Journal of Inorganic Chemistry*, (2008) 883-889.
- [21] E. Brun, F. Barreau, G. Veronesi, B. Fayard, S. Sorieul, C. Chaneac, C. Carapito, T. Rabilloud, A. Mabondzo, N. Herlin-Boime, M. Carriere, Titanium dioxide nanoparticle

impact and translocation through ex vivo, in vivo and in vitro gut epithelia, *Particle and fibre toxicology*, 11 (2014) 13.

[22] M. Dorier, E. Brun, G. Veronesi, F. Barreau, K. Pernet-Gallay, C. Desvergne, T. Rabilloud, C. Carapito, N. Herlin-Boime, M. Carriere, Impact of anatase and rutile titanium dioxide nanoparticles on uptake carriers and efflux pumps in Caco-2 gut epithelial cells, *Nanoscale*, 7 (2015) 7352-7360.

[23] P.B. Stathopoulos, G.A. Scholz, Y.M. Hwang, J.A. Rumfeldt, J.R. Lepock, E.M. Meiering, Sonication of proteins causes formation of aggregates that resemble amyloid, *Protein science*, 13 (2004) 3017-3027.

[24] J.S. Taurozzi, V.A. Hackley, M.R. Wiesner, Ultrasonic dispersion of nanoparticles for environmental, health and safety assessment--issues and recommendations, *Nanotoxicology*, 5 (2011) 711-729.

[25] S. Frelon, T. Douki, J.L. Ravanat, J.P. Pouget, C. Tornabene, J. Cadet, High-performance liquid chromatography--tandem mass spectrometry measurement of radiation-induced base damage to isolated and cellular DNA, *Chemical research in toxicology*, 13 (2000) 1002-1010.

[26] J.L. Ravanat, T. Douki, P. Duez, E. Gremaud, K. Herbert, T. Hofer, L. Lasserre, C. Saint-Pierre, A. Favier, J. Cadet, Cellular background level of 8-oxo-7,8-dihydro-2'-deoxyguanosine: an isotope based method to evaluate artefactual oxidation of DNA during its extraction and subsequent work-up, *Carcinogenesis*, 23 (2002) 1911-1918.

[27] M.W. Pfaffl, A. Tichopad, C. Prgomet, T.P. Neuvians, Determination of stable housekeeping genes, differentially regulated target genes and sample integrity: BestKeeper--Excel-based tool using pair-wise correlations, *Biotechnology letters*, 26 (2004) 509-515.

[28] M.W. Pfaffl, G.W. Horgan, L. Dempfle, Relative expression software tool (REST) for group-wise comparison and statistical analysis of relative expression results in real-time PCR, *Nucleic acids research*, 30 (2002) e36.

- [29] J. Forstner, G.G. Forstner, *Gastrointestinal mucus*, in: J. LR (Ed.) *Physiology of the gastrointestinal tract*. 3rd edn, Raven Press, New York, 1994, pp. 1255–1283.
- [30] X.X. Chen, B. Cheng, Y.X. Yang, A. Cao, J.H. Liu, L.J. Du, Y. Liu, Y. Zhao, H. Wang, Characterization and preliminary toxicity assay of nano-titanium dioxide additive in sugar-coated chewing gum, *Small*, 9 (2013) 1765-1774.
- [31] E. Frohlich, E. Roblegg, Models for oral uptake of nanoparticles in consumer products, *Toxicology*, 291 (2012) 10-17.
- [32] J.J. Powell, N. Faria, E. Thomas-McKay, L.C. Pele, Origin and fate of dietary nanoparticles and microparticles in the gastrointestinal tract, *Journal of autoimmunity*, 34 (2010) J226-233.
- [33] C. McCracken, P.K. Dutta, W.J. Waldman, Critical assessment of toxicological effects of ingested nanoparticles, *Environmental Science-Nano*, 3 (2016) 256-282.
- [34] H. Shi, R. Magaye, V. Castranova, J. Zhao, Titanium dioxide nanoparticles: a review of current toxicological data, *Particle and fibre toxicology*, 10 (2013) 15.
- [35] M. Skocaj, M. Filipic, J. Petkovic, S. Novak, Titanium dioxide in our everyday life; is it safe?, *Radiology and oncology*, 45 (2011) 227-247.
- [36] K. Gerloff, C. Albrecht, A.W. Boots, I. Förster, R.P.F. Schins, Cytotoxicity and oxidative DNA damage by nanoparticles in human intestinal Caco-2 cells *Nanotoxicology* 3(2009) 355–364.
- [37] K. Gerloff, I. Fenoglio, E. Carella, J. Kolling, C. Albrecht, A.W. Boots, I. Forster, R.P. Schins, Distinctive toxicity of TiO₂ rutile/anatase mixed phase nanoparticles on Caco-2 cells, *Chemical research in toxicology*, 25 (2012) 646-655.
- [38] A. Lesniak, F. Fenaroli, M.P. Monopoli, C. Aberg, K.A. Dawson, A. Salvati, Effects of the presence or absence of a protein corona on silica nanoparticle uptake and impact on cells, *ACS nano*, 6 (2012) 5845-5857.

- [39] M.P. Monopoli, C. Aberg, A. Salvati, K.A. Dawson, Biomolecular coronas provide the biological identity of nanosized materials, *Nature nanotechnology*, 7 (2012) 779-786.
- [40] N.P. Mortensen, G.B. Hurst, W. Wang, C.M. Foster, P.D. Nallathamby, S.T. Retterer, Dynamic development of the protein corona on silica nanoparticles: composition and role in toxicity, *Nanoscale*, 5 (2013) 6372-6380.
- [41] L.G. Hernandez, H. van Steeg, M. Luijten, J. van Benthem, Mechanisms of non-genotoxic carcinogens and importance of a weight of evidence approach, *Mutation research*, 682 (2009) 94-109.
- [42] G. Vales, L. Rubio, R. Marcos, Long-term exposures to low doses of titanium dioxide nanoparticles induce cell transformation, but not genotoxic damage in BEAS-2B cells, *Nanotoxicology*, 9 (2015) 568-578.
- [43] J. Susewind, C.D. Carvalho-Wodarz, U. Repnik, E.M. Collnot, N. Schneider-Daum, G.W. Griffiths, C.M. Lehr, A 3D co-culture of three human cell lines to model the inflamed intestinal mucosa for safety testing of nanomaterials, *Nanotoxicology*, 10 (2016) 53-62.

Table 1. RT-qPCR analysis of the mRNA expression of DNA repair proteins, redox enzymes and proteins implicated in endoplasmic reticulum stress^a

	A12 6h	NM105 6h	E171 6h	A12 48h	NM105 48h	E171 48h
<i>DNA repair</i>						
OGG1	0.90±0.14	0.77±0.16	1.06±0.18	0.94±0.71	1.63±1.11	1.81±1.43
APE1	1.44±0.49	1.00±0.38	0.89±0.30	0.99±0.25	1.08±1.17	0.87±0.31
PARP1	1.13±0.30	0.92±0.24	0.87±0.20	1.19±0.44	1.13±0.47	1.15±0.53
LIG3	1.07±0.29	0.88±0.21	0.70±0.50	1.05±0.37	1.03±0.40	1.30±0.48
XRCC1	1.19±0.36	0.93±0.32	2.52±2.53	1.57±1.02	1.54±0.96	1.89±1.30
PCNA	1.40±0.35	0.88±0.20	1.17±0.27	1.06±0.36	1.06±0.36	1.26±0.76
GADD45	1.27±0.44	0.71±0.24	0.74±0.27	1.66±0.62	1.86±0.70*	1.83±1.05
<i>oxidative balance</i>						
SOD1	1.20±0.32	1.63±0.63	1.22±0.63	0.66±0.34	0.92±0.44	0.49±0.15*
SOD2	1.92±1.49	2.04±1.76	1.40±1.24	0.68±0.17*	1.04±0.47	1.00±0.53
CAT	0.99±0.29	1.44±0.53	0.85±0.41	1.14±0.57	0.96±0.49	0.96±0.42
GSR	0.75±0.34	1.08±0.43	0.81±0.40	1.15±0.69	0.70±0.35	1.11±0.34
NRF2	1.04±0.27	1.21±0.45	1.01±0.65	0.97±0.49	0.86±0.70	1.07±0.57
<i>endoplasmic reticulum stress</i>						
IRE1	0.78±0.19	1.03±0.26	0.92±0.54	0.93±0.67	1.24±1.20	1.57±1.50
SXBP1	0.95±0.35	1.04±0.40	1.43±0.61	1.14±1.31	1.19±0.84	1.61±1.47
GRP78	0.88±0.20	0.94±0.19	1.09±0.41	1.24±1.21	1.15±0.63	1.51±0.93
ATF6	1.09±0.23	0.93±0.31	1.27±0.87	0.91±0.98	1.08±0.68	1.06±0.85

^aImpact on gene expression of selected genes, obtained by RT-qPCR from Caco-2/HT29-MTX cells exposed for 6 h or 48 h to 50 µg/mL of TiO₂ particles. Results are expressed as fold-increase above the control (unexposed cells) and expressed as average ± standard deviation. *p<0.05 (indicated in bold), exposed vs control, n=3.

Figure 1. Proportion of Caco-2 and HT29-MTX cells in the co-culture. FACS analysis of Caco-2-GFP/HT29-MTX co-culture immediately after seeding (A), or 6 h (B), or 48 h (C) or 72 h (D) after seeding. Proportion of green fluorescent cells to non-fluorescent cells (E), reflecting the proportions of Caco-2-GFP and HT29-MTX cells. Results are expressed as percentage (%) of each cell type (Caco-2-GFP: white and HT29-MTX: grey), presented as average \pm standard deviation, * $p < 0.05$, 6 h or 48 h or 72 h vs. time point 0, $n=3$.

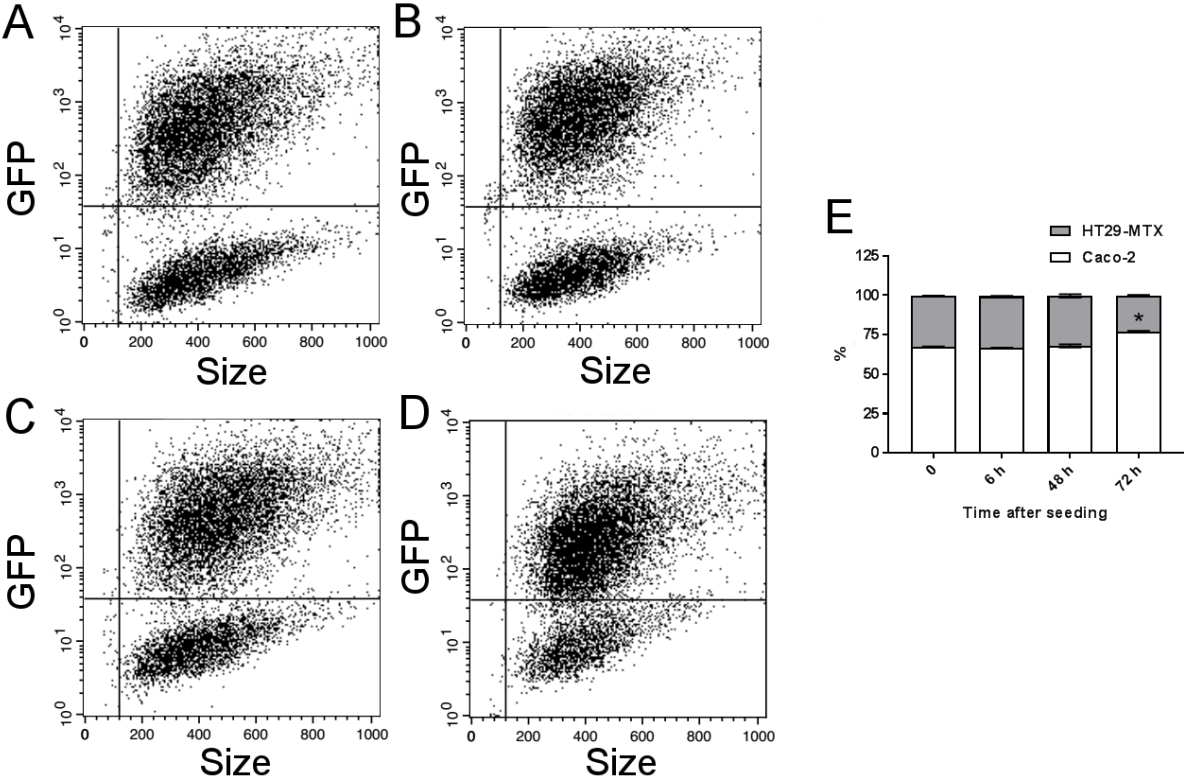


Figure 2. Impact of TiO₂ particles on cell viability. Cell metabolic activity, reflecting viability, was probed with the MTT assay in Caco-2/HT29-MTX cells after 6h and 48h of exposure to NM105 (A) and E171 food additive (B) at 20, 50, 100 and 200 µg/mL. Results are expressed as percentage (%) of the value obtained in control cells (unexposed cells), presented as average ± standard deviation, n=3.

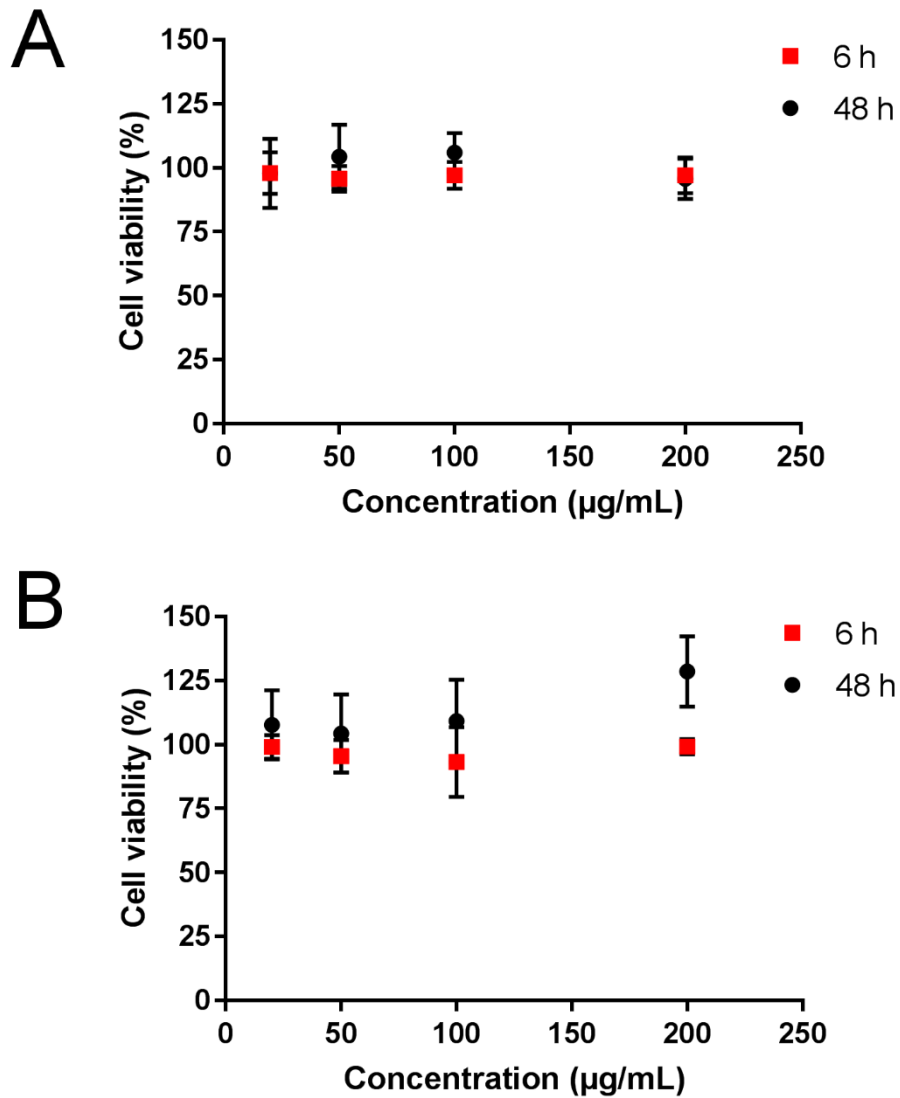


Figure 3. Intracellular ROS content. ROS content was measured using DCFH-DA assay, in Caco-2/HT29-MTX co-culture exposed for 6 h, 24 h or 48 h to 50 $\mu\text{g/mL}$ of A12 or NM105, or E171 (A), or to 10, 50 and 100 $\mu\text{g/mL}$ of E171 (B). As positive control, cells were exposed for 24 h to 250 μM of KBrO_3 . ROS level is expressed as fold-change compared to ROS level in control cells. Average \pm standard deviation. * $p < 0.05$, exposed vs. control, # $p < 0.05$, 50 or 100 $\mu\text{g/mL}$ E171 vs. 10 $\mu\text{g/mL}$ E171 $n = 4$.

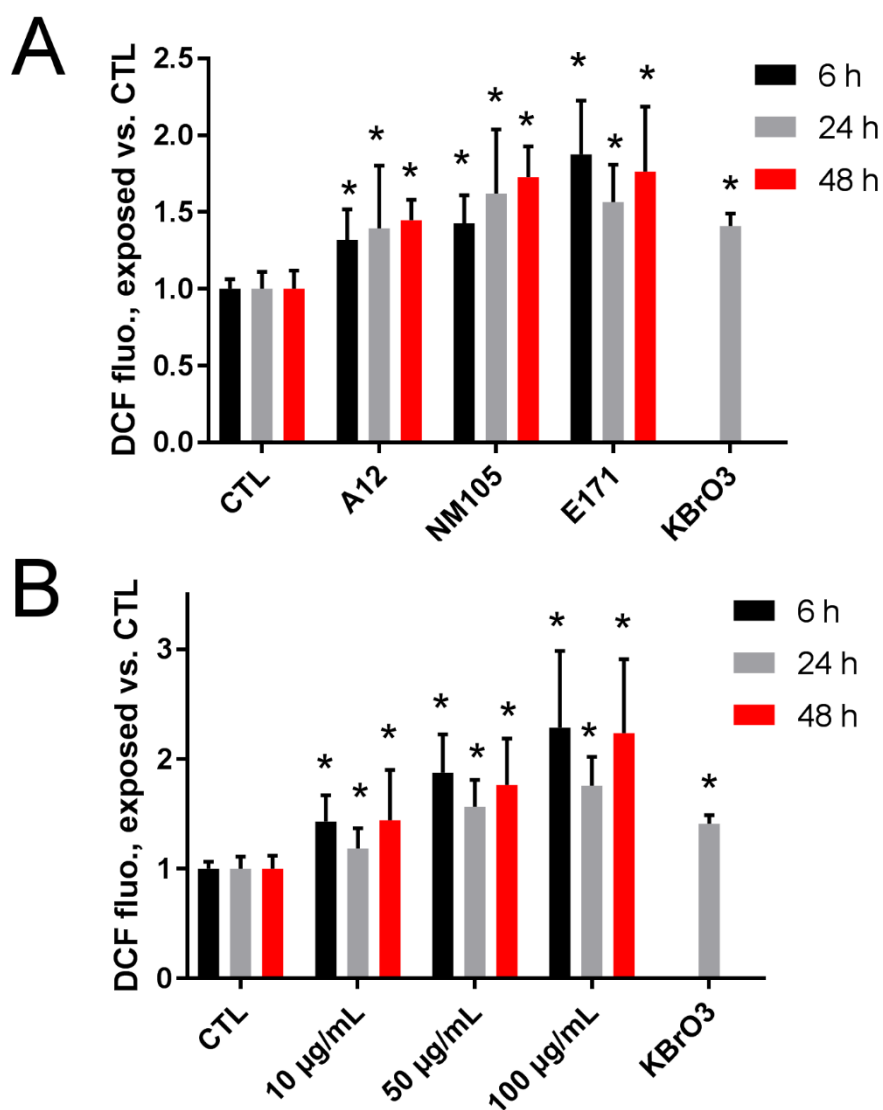


Figure 4. DNA damage caused by TiO₂ particles, assessed using alkaline and Fpg-modified comet assay. Cells were exposed to 50 µg/mL A12 or NM105 or E171 for 24 h, then DNA damage was investigated via comet assay. % tail DNA was measured; the alkaline version of this assay probes strand breaks and alkali-labile sites (SBs+ALB) the Fpg-modified version of this assay probes strand breaks, alkali-labile sites and Fpg-sensitive sites (SBs+ALB+Fpg), the level of Fpg-sensitives sites is calculated by subtracting % tail DNA obtained in the alkaline version of the assay from % tail DNA obtained in the Fpg-modified version (Net Fpg). Ribo/UVA: positive control for comet-Fpg assay, cells treated with riboflavin then exposed to UVA. MMS: positive control for alkaline comet assay, cells treated with 30 µg/mL of methane methylsulfonate for 24 h. *p < 0.05, exposed vs. control, n=3.

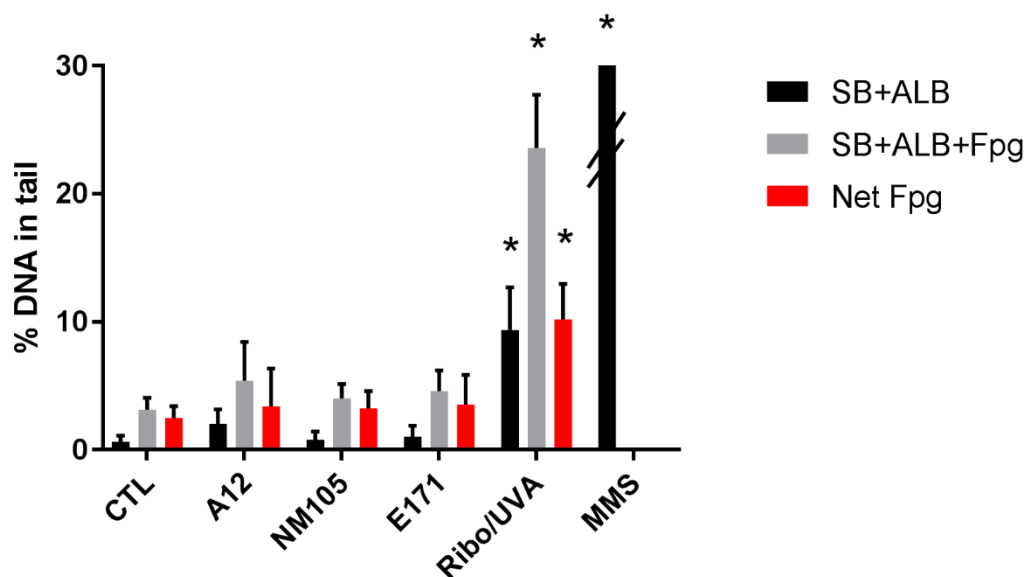


Figure 5. Double strand break level was measured via 53BP1 immunostaining and foci count, using high content analysis. Double strand breaks in DNA were assessed via immunostaining and counting of 53BP1 foci, in control cells (A), cells exposed to 50 μ M of etoposide (B), or 50 μ g/mL A12 (C) or NM105 (D) or E171 (E) for 24 h. Blue fluorescence corresponds to staining of nuclei, and green fluorescence corresponds to staining of 53BP1. Numbers of foci are summarized in graph (F). Results are expressed as average \pm standard deviation. * $p < 0.05$, exposed vs. control, $n=5$.

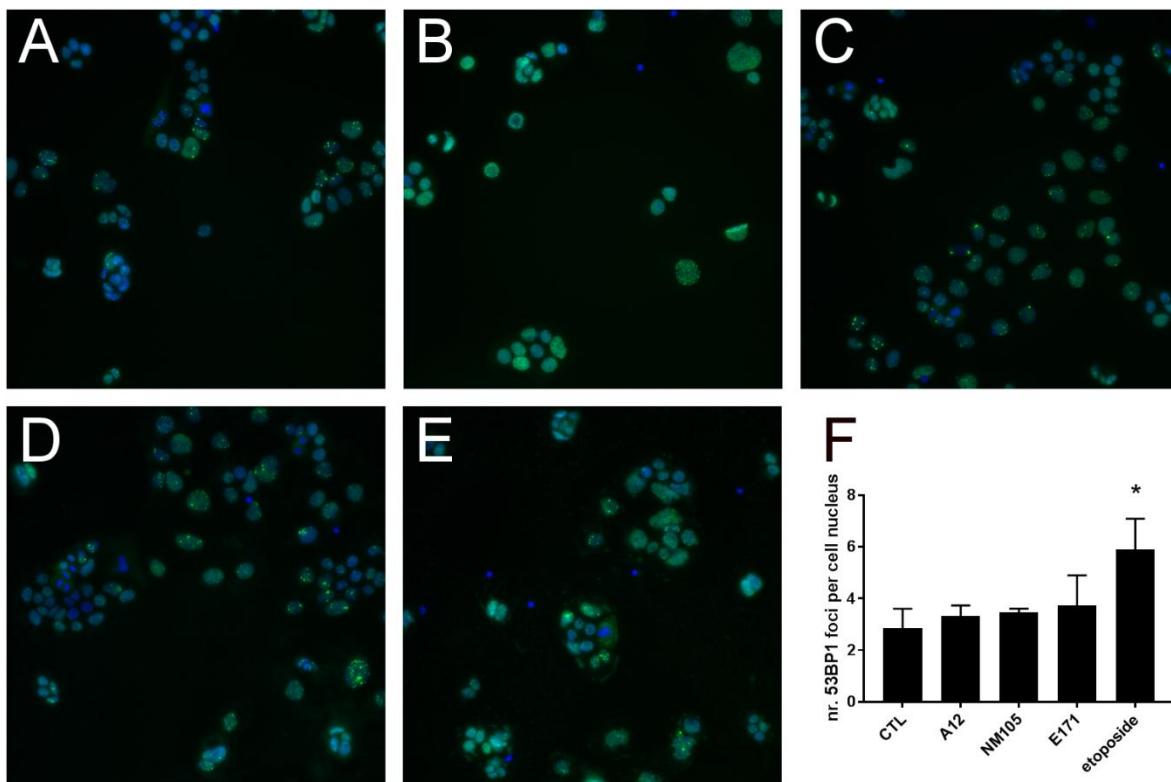
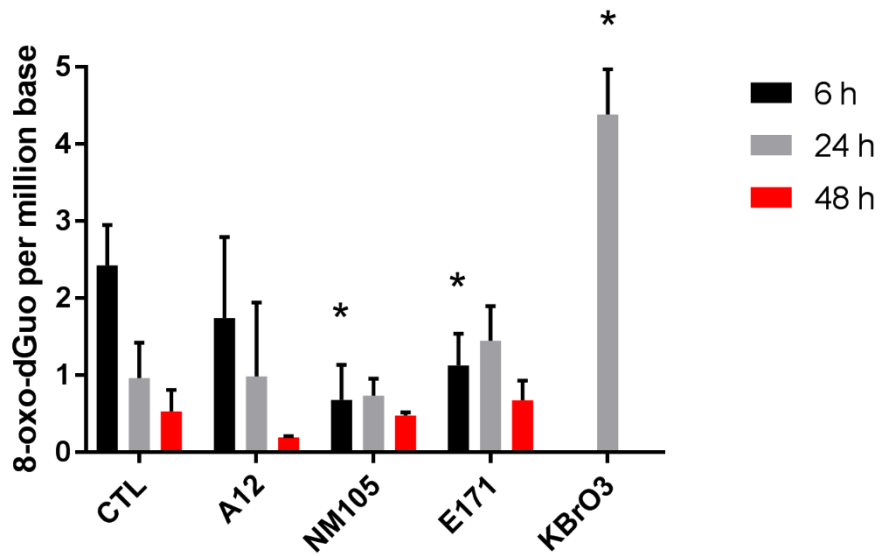


Figure 6. 8-oxo-dGuo level, measured via HPLC-MS/MS. Cells were exposed to 50 $\mu\text{g}/\text{mL}$ A12 or NM105 or E171 for 6 h, 24 h or 48 h. As positive control, cells were exposed for 24 h to 250 μM of KBrO_3 . Results are expressed as average \pm standard deviation. * $p < 0.05$, exposed vs. control, $n = 3$.



9. Supplementary materials

Table S1. Interference of E171 with MTT assay^a

	No centrifugation			After centrifugation		
	A570	A650	A570-A650	A570	A650	A570-A650
0	0.295	0.102	0.193	0.124	0.060	0.064
1 mg/mL	1.363	1.137	0.226	0.130	0.074	0.056
2 mg/mL	1.993	1.658	0.335	0.128	0.075	0.053
3 mg/mL	2.203	1.841	0.362	0.122	0.076	0.046
4 mg/mL	2.438	1.971	0.467	0.170	0.108	0.062
5 mg/mL	2.625	2.099	0.526	0.394	0.252	0.142

^aInterference with MTT assay was assessed as follows: control Caco2/HT29-MTX cells (not exposed to E171 or TiO₂-NPs) were incubated with MTT for 1 h at 37°C. The exposure medium was then replaced by 100 µL of DMSO and agitated for 5 min in order to lyse the cells and release formazan. After agitation, this solution was mixed with 0, 1, 2, 3, 4, or 5 mg/mL of E171. Absorbance was measured at 570 nm (A570) and corrected via subtraction of background absorbance at 650 nm (A650). These values are indicated in the columns “No centrifugation”. The plate was then centrifuged for 5 min at 200 rcf, and 50 µL of each well was transferred to a clean well. Again, absorbance was measured at 570 nm (A570) and corrected via subtraction of background absorbance at 650 nm (A650). These values are indicated in the columns “After centrifugation”. In the non-centrifuged wells, A570-A650 gradually increases with increasing concentrations of E171. Conversely, when centrifugation was applied, A570-A650 did not increase. We therefore conclude that using an additional step of centrifugation at the end of the classical MTT protocol, is sufficient to avoid interference of E171. This conclusion is valid for concentrations of E171 from 1 to 3 mg/mL.

Table S2. Interference of TiO₂ with DCFH-DA^a

	Caco-2/HT29-MTX		No cell
	No DCFH-DA	DCFH-DA	DCFH-DA
Control	17.2±0.3	11643.2±937.7	2.6±0.1
A12 50 µg/mL	14.6±0.3	11992.4±1213.5	3.3±0.0
P25 50 µg/mL	14.6±0.9	16646.6±607.0	3.4±0.2
E171 10 µg/mL	17.1±1.3	14673.4±1454.1	2.7±0.2
E171 50 µg/mL	16.5±0.5	14940.1±1697.9	3.2±0.3
E171 100 µg/L	14.1±2.3	18843.0±2751.2	4.1±0.1

^aPotential interference of TiO₂ particles with the DCFH-DA assay was tested by measurement of DCF fluorescence, either in cells exposed to particles but not to DCFH-DA (“Caco-2/HT29-MTX; No DCFH-DA”), or in cells exposed to particles and to DCFH-DA, using the same protocol as in Figure 2 (“Caco-2/HT29-MTX; DCFH-DA”). Fluorescence was also measured on particle suspensions to which DCFH-DA was added (“No cell; DCFH-DA”). Fluorescence was measured with excitation at 480 nm and emission at 530 nm, cutoff 515 nm.

Table S3. Sequences of qPCR primers

	Forward primer	Reverse primer
Oxidative stress		
CAT	5'-AGC-TTA-GCG-TTC-ATC-CGT-GT-3'	5'-TCC-AAT-CATC-CGT-CAA-AAC-A-3'
GSR	5'-GAT-CCC-AAG-CCC-ACA-ATA-GA-3'	5'-CTT-AGA-ACC-CAG-GGC-TGA-CA-3'
SOD1	5'-AGG-GCA-TCA-TCA-ATT-TCG-AG-3'	5'-ACA-TTG-CCC-AAG-TCT-CCA-AC-3'
SOD2	5'-TCC-ACT-GCA-AGG-AAC-AAC-AG-3'	5'-TCT-TGC-TGG-GAT-CAT-TAG-GG-3'
NRF2	5'-CAG-TCA-GCG-ACG-GAA-AGA-GT-3'	5'-ACC-TGG-GAG-TAG-TTG-GCA-GA-3'
Endoplasmic reticulum stress		
GRP78	5'-GGT-GAA-AGA-CCC-CTG-ACA-AA-3'	5'-GTC-AGG-CGA-TTC-TGG-TCA-TT-3'
CHOP	5'-TGG-AAG-CCT-GGT-ATG-AGG-AC-3'	5'-TGT-GAC-CTC-TGC-TGG-TTC-TG-3'
IRE1	5'-AGA-GAG-GCG-GGA-GAG-CCG-TG-3'	5'-CGA-GGA-GGT-GGG-GGA-AGC-GA-3'
sXBP1	5'-GCA-GGT-GCA-GGC-CCA-GTT-GT-3'	5'-TGG-GTC-CAA-GTT-GTC-CAG-AAT-GC-3'
ATF-6	5'-CCA-GCA-GCA-CCC-AAG-ACT-CAA-ACA-3'	5'-GTG-TGA-CTC-CCC-CAG-CAA-CAG-C-3'

Figure S1. Interference of TiO₂ particles with the MTT assay. TiO₂ may interfere with the MTT assay due to their opacity, which impairs proper absorbance measurement. To get rid of this optical interference, plates were centrifuged to allow particles to settle down. Then 50 μ L of supernatant from each well was transferred to a clean plate, absorbance was measured and normalized to the values obtained in controls (unexposed cells). Measurement was performed on Caco-2 (A), HT29-MTX (B) or the Caco-2/HT29-MTX coculture (C), exposed to 25-200 μ g/mL of E171.

